Volterra Series Estimation of Transient Soot Emissions from a Diesel Engine

Rahul Ahlawat, Jonathan R. Hagena, Zoran S. Filipi, Jeffrey L. Stein and Hosam K. Fathy

***Abstract*— This paper describes the development of a Volterra series model for predicting transient soot emissions from a diesel engine with fuel flow rate and engine speed as the two inputs to the model. These two signals are usually available as outputs of the power management controller in diesel hybrids. Therefore, an accurate offline estimation of the transient soot emissions using these signals is instrumental in optimizing the control strategy for both fuel economy and emissions. In order to develop the model, transient soot data are first collected by Engine-in-the-loop experiments of conventional and hybrid vehicles. The data are then used to construct a third-order multiple-input single-output (MISO) Volterra series to successfully model this system. Parametric complexity of the model is reduced using proper orthogonal decomposition (POD), and the model is validated on various datasets. It is shown that the prediction accuracy of transient soot, both qualitatively and quantitatively, significantly improves over the steady-state maps, while the model still remains computationally efficient for systems level work.**

I. Introduction

This paper presents a Volterra series model for the transient soot emissions produced by a diesel engine, with fuel flow rate and engine speed as the two inputs to the model. The model is intended for the purpose of designing powertrain-level supervisory controllers that minimize transient soot emissions, among other possible objectives. This can be particularly important in the context of hybrid diesel propulsion systems. While such systems offer more flexibility in controlling their engines as compared to the conventional powertrains, optimizing their supervisory control for fuel economy alone can lead to frequent and sharp load increases, thereby significantly penalizing soot emissions [1]. Our overarching goal, therefore, is to develop a transient soot emission model that meets three key criteria. First, it must accurately capture the impact of powertrain transients on the resulting transient soot emissions. Second, it must be simple enough to enable control system design. Third, the model's inputs should ideally consist of quantities that are easy to simulate or control, such as engine speed and fuel flow rate.

Quasi steady state models based on steady-state emission maps have been used in the literature for control-oriented modeling but they fail to capture transient soot accurately, especially the spikes during tip-in operations [2], [3], [4]. More detailed models exist in the literature that capture transient soot formation by simulating the combustion events using computational fluid dynamics (CFD) [5], phenomenological methods [6], [7], [2], [8], [9], heuristic macro-parameter approaches [10] or using black box models such as artificial neural networks [11]. However, these approaches require a number of inputs to the model often not available to the control engineers involved with vehicle-level control development. Also, simulating combustion can sometimes be prohibitively slow in the context of system work [6].

In this work we seek to develop a model capable of predicting instantaneous soot at the exhaust manifold of a diesel engine, subjected to the transient loads emulating the operation in a vehicle following the FTP-75 city cycle, with just two inputs: engine speed (ω_e) and fuel flow rate $(\dot{m})$. Both of these signals are usually the outputs of the powertrain supervisory control, and this model will enable the control system development for soot reduction without simulating the combustion dynamics. Although this work is focused on modeling the diesel engine soot emissions during the FTP-75 city cycle, the techniques and analysis presented here can be generalized to other engines with different inputs and outputs. Experimental data for transient soot is recorded using Engine-in-the-loop (EIL) experiments of conventional and hybrid diesel vehicles. The data are analyzed for statistical and spectral properties and system identification techniques are then used to fit a model to the inputs and the soot output. It is shown that a multiple-input single-output (MISO) Volterra series with low parametric complexity can furnish good estimates, both qualitatively and quantitatively. The model is then validated on a number of different datasets, and a comparison with steady-state models is presented.

The rest of the paper is organized such that section 2 describes the test setup for recording the data and their analysis is presented in section 3. Section 4 develops the Volterra series model used for the identification of transient soot. Section 5 presents the model validation results, and finally the conclusions are drawn in section 6.

II. Experimental Methodology

The transient soot data are recorded using Engine-in-the-loop (EIL) testing. The block diagram of the EIL setup used is shown in Fig. 1. The engine used in this investigation is a 6.0L V-8 direct-injection diesel engine. Driver, transmission and vehicle models are simulated on the real-time (RT) platform. These models accurately capture the desired dynamics while being numerically efficient to run in real-time [12]. Along with the EIL simulation of the conventional vehicle, models for three other powertrain configurations are

Address all correspondence to Hosam Fathy (hfathy@umich.edu).

Rahul Ahlawat is a PhD candidate at the University of Michigan, Ann Arbor. Dr. Hosam K. Fathy, Prof. Zoran S. Filipi, and Prof. Jeffrey L. Stein are with the Department of Mechanical Engineering, University of Michigan, Ann Arbor. Dr. Jonathan Hagena is with PACCAR Technical Center, Mt. Vernon, WA.

978-1-4244-8218-4/10/$26.00 ©2010 IEEE

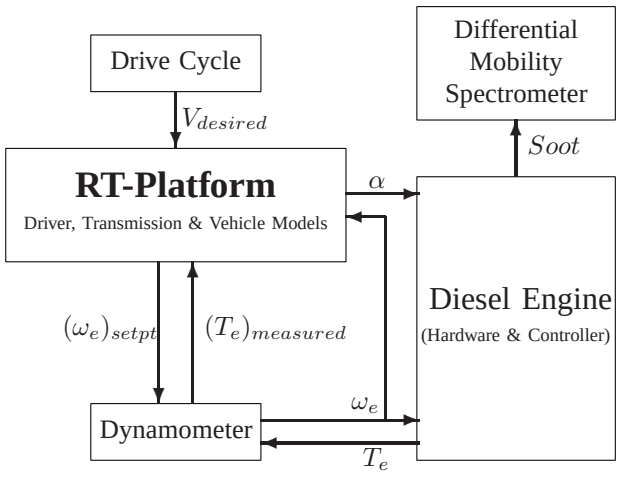

Fig. 1. EXPERIMENTAL SETUP FOR EIL TESTING

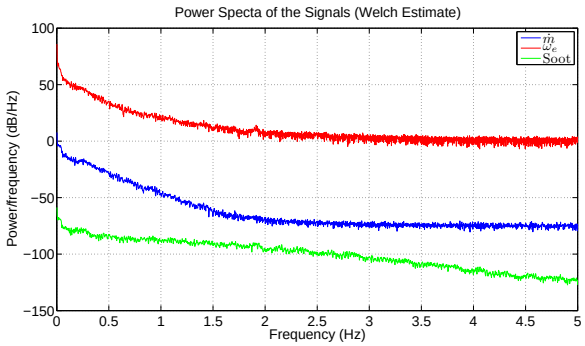

Fig. 2. SAMPLE SIGNAL SPECTRA

also implemented; virtually downsized engine (scaling down the torque measurement of the engine to emulate a smaller engine), parallel electric hybrid [13], and series hydraulic hybrid [14]. These different configurations subject the engine to different operating points and transient loads, generating data that cover a wide range on the engine map. A downsized engine results in much harsher transients, series hydraulic hybrid subjects the engine to a lot of steady-state operation, whereas conventional vehicle and parallel electric vehicles operate the engine at different transient profiles. Multiple runs are made for each configuration in order to have separate datasets for identification and validation.

Due to the forward-looking nature of the vehicle model, the driver model issues throttle and brake commands to follow the vehicle velocity on the FTP-75 city cycle. Model causality is selected such that the torque converter model commands speed to the engine, as speed is easier to control than the engine torque. The engine speed is controlled using a 330kW AC Dynamometer. The measured engine torque is fed to the torque-converter model to enable closed-loop drive-cycle simulation. The driver's throttle command (α) is communicated to the engine controller, which is then converted into an equivalent fuel flow rate and commanded to the engine. Thus during the EIL simulation, the engine subsystem is controlled by two exogenous inputs, ω_e and $\dot{m}$ (or α).

The transient soot data are recorded using a differential mobility spectrometer (DMS). This instrument measures the number of particles and their spectral weighting in the 5nm to 1000nm size range with a time response of 200ms [15]. These aerosol size spectral data are then converted into particulate mass. Agglomerates formed during diesel combustion are non-spherical and therefore their mass does not correlate with the cube of the particle diameter. Similarly, the constituents of the particles change as the diameter varies and consequently there is a non-linear relationship between particle density and diameter. To convert particle spectral density to mass, a relationship has been suggested by the manufacturer [3]. The spectral diameter (D_p) in nanometers is divided into bins, density of the particles within each bin is assumed to be constant and then the mass of the particles in each bin is determined by

$$\text{Particle Mass} = 6.95 \times 10^{-3} \cdot D_p^{2.34} \cdot \text{Number of particles} \quad (1)$$

After the particle mass is calculated for each bin, the total mass is found by summing the masses in each bin and dividing by the number of bins per decade

$$\text{Total Mass} = \frac{\sum_{\text{Bins}} \text{Mass}}{\text{Bins/Decade}} [kg/m^3] \quad (2)$$

This summation is used as an approximation that accounts for integration over a logarithmic scale. The instantaneous soot emissions are then obtained by multiplying this mass per unit volume with the volume flow rate. More details on the experimental setup and the models used can be found in [1] and [12].

III. STATISTICAL AND SPECTRAL DATA ANALYSIS

In this section we analyze the recorded data for noise, coherence and cross-correlations. The input ($\dot{m}$ & ω_e) and output ($Soot$) data from EIL testing are sampled at 10Hz for the entire FTP-75 city cycle. This soot data should not be confused with the cylinder's cycle-to-cycle soot emission, which has dynamics of a much faster timescale. The soot data here is the engine's soot emission per unit time, as measured from the exhaust pipe, and has much slower dynamics due to the presence of the turbocharger and the exhaust manifold, and hence a sample rate of 10Hz suffices. The data obtained are first analyzed for high-frequency noise. Fig. 2 shows the average power spectra for the inputs and the output of a sample dataset. It is observed that each of these signals primarily consist of low frequency components, and are devoid of high frequency noise. There is no prefiltering to prevent aliasing, because at frequencies near the Nyquist frequency, signals are almost 50dB lower than those in the low frequency range.

Coherence functions can be used to investigate the degree to which a given output can be linearly predicted from all

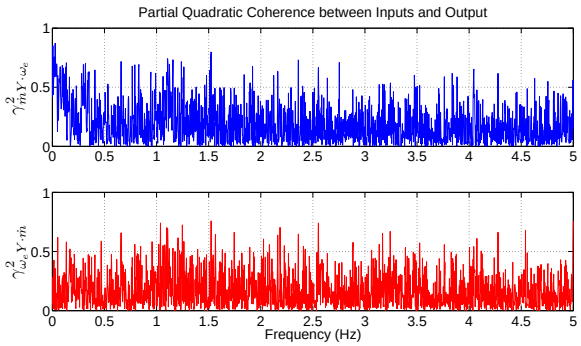

Fig. 3. SAMPLE COHERENCE SPECTRUM BETWEEN INPUTS AND OUTPUT

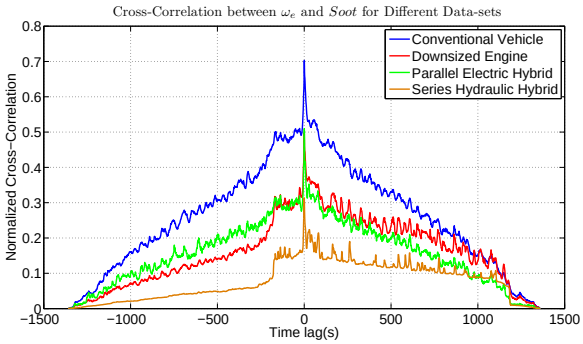

Fig. 4. CROSS-CORRELATION BETWEEN ω_e AND $Soot$

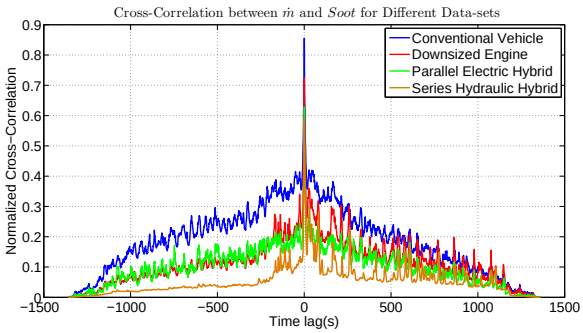

Fig. 5. CROSS-CORRELATION BETWEEN $\dot{m}$ AND $Soot$

of the system inputs and to determine the frequencies over which a linear model can accurately characterize the system dynamics. Quadratic coherence always takes on a value in the interval $[0, 1]$, with a value close to 1 if there is a linear response between the input and the output, serving as a form of correlation function in the frequency domain. Regions of low coherence indicate insufficient input power in that frequency range, significant system nonlinearities, noise, or contributions from unmeasured inputs [16]. Partial coherence provides an estimate of the linear relationship between one input and one output for multiple-input multiple-output (MIMO) systems. These estimates are equivalent to ordinary coherence estimates after the effects of all other inputs have been removed from both the input and output of interest [16]. Let the output of our system ($Soot$) be represented by Y, and the cross-spectrum between two signals x and y be represented by G_{xy}. Then the partial coherence functions for our system with two inputs and one output are given by

$$\gamma^2_{\dot{m}Y\cdot\omega_e}(f) = \frac{|G_{\dot{m}Y\cdot\omega_e}(f)|^2}{G_{\dot{m}\dot{m}\cdot\omega_e}(f)\cdot G_{YY\cdot\omega_e}(f)} \tag{3}$$

$$\gamma^2_{\omega_e Y\cdot\dot{m}}(f) = \frac{|G_{\omega_e Y\cdot\dot{m}}(f)|^2}{G_{\omega_e\omega_e\cdot\dot{m}}(f)\cdot G_{YY\cdot\dot{m}}(f)} \tag{4}$$

where the residual spectrum, $G_{xy\cdot z}$, is defined as

$$G_{xy\cdot z}(f) = G_{xy}(f)\cdot\left[1 - \frac{G_{xz}(f)\cdot G_{zy}(f)}{G_{zz}(f)\cdot G_{xy}(f)}\right] \tag{5}$$

These partial coherence functions are plotted in Fig. 3 for sample signals. Both of these partial coherence plots indicate strong nonlinear relationships between $\dot{m}$ & $Soot$, and ω_e & $Soot$, for all frequencies. Hence our system warrants the use of a non-linear model structure for identification.

The correlation between the inputs and the output is analyzed next. Fig. 4 shows the cross-correlation of $Soot$ with ω_e, and Fig. 5 shows the same function for $Soot$ and $\dot{m}$, at different time lags. Both graphs indicate that the correlations change for different data-sets (conventional vehicle, downsized engine, parallel electric, and series hydraulic) making them valuable for the validation of the proposed model. Also, since cross-correlations decrease with time, the system exhibits fading memory and hence a finite order model can be used. In terms of time-history, strong correlations are exhibited only around zero lag. Fig. 6 shows the magnified view of the correlation coefficients for a sample dataset. The peak correlation of the transient soot with the inputs is not at zero lag but slightly delayed, due to the slower exhaust manifold dynamics. Also, higher correlations are exhibited with the time-lag of less than one second, and hence the inputs in this window will be used for identification.

IV. TRANSIENT SOOT VOLTERRA MODELS

This section presents the development of the proposed transient soot emission model using the Volterra series. Soot formation involves complex combustion processes that are inherently non-linear [2], [17], and hence these emissions are best modeled using non-linear system identification techniques. The Volterra series is a non-linear functional series with polynomial basis functions, and can be interpreted as a

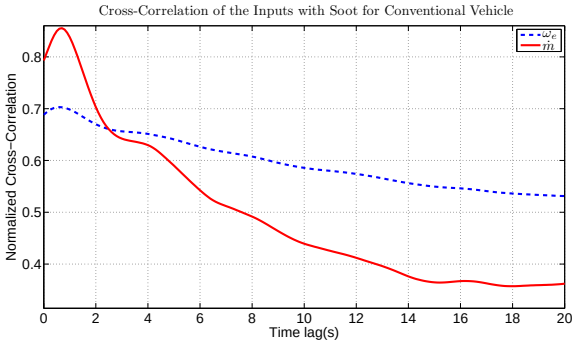

Fig. 6. TIME-LAG FOR PEAK CROSS-CORRELATIONS

direct generalization of the linear convolution integral [18]. For a single-input (u), single-output(y) (SISO) system, it can be expressed as

$$y(t) = \sum_{n=1}^{\infty} y_n(t) \tag{6}$$

where $y_n(t)$ is the 'n th-order output' of the system

$$y_n(t) = \int_{-\infty}^{\infty} \cdots \int_{-\infty}^{\infty} h_n^u(\tau_1, \tau_2, \ldots, \tau_n) \prod_{i=1}^{n} u(t-\tau_i) \mathrm{d}\tau_i, \quad n > 0 \tag{7}$$

where $h_n^u(\tau_1, \tau_2, \ldots, \tau_n)$ is called the 'n th-order Kernel' or 'n th-order impulse response function'. If $n = 1$, this reduces to the familiar linear convolution integral.

A discrete-time equivalent of Eqn. 6 can be expressed as

$$y(k) = \sum_{n=1}^{\infty} y_n(k) \tag{8}$$

where

$$y_n(k) = \sum_{-\infty}^{\infty} \cdots \sum_{-\infty}^{\infty} h_n^u(\tau_1, \tau_2, \ldots, \tau_n) \prod_{i=1}^{n} u(k-\tau_i), \quad n > 0, k \in \mathbf{Z} \tag{9}$$

Boyd and Chua [19] showed that this discrete time Volterra series can be approximated to the desired accuracy, if the non-linear operator is causal, continuous, time-invariant, and has fading memory, and if the inputs are bounded. This is the case for a wide-class of non-linear systems, unless they contain dynamic behaviors such as limit cycles, sub-harmonics, or chaos [20], [21]. An immediate consequence is that the higher order terms can be neglected in such a way that only the first M Volterra kernels need to be taken into account, where M is the order of the resulting model. Since the desired representation is stable, the elements of $h_n^u(\tau_1, \tau_2, \ldots, \tau_n)$ with $\tau_l > \varepsilon_n (\forall l \in 1, \ldots, n)$ can be ignored [22], and Eqn 8 simplifies to

$$y(k) = \sum_{n=1}^{M} \sum_{\tau_1=0}^{\varepsilon_n} \cdots \sum_{\tau_n=0}^{\varepsilon_n} h_n^u(\tau_1, \tau_2, \ldots, \tau_n) \prod_{i=1}^{n} u(k-\tau_i) \tag{10}$$

Once the Volterra series is established, the problem at hand reduces to finding the Volterra kernels. The main drawback here is that the kernels are, in principle, non-parameterized functions whose measurement is possible only if their individual contributions can be separated from the total system response [23]. If the elements of all the Volterra kernels,

$$\mathbf{H} = \{h_1, h_2, \ldots, h_m\} \text{ where } m = \frac{(\varepsilon_n + M + 1)!}{(\varepsilon_n + 1)! M!} - 1 \tag{11}$$

are treated as individual parameters to be estimated, and since the Volterra model is linear in these parameters, classical estimation algorithms can be applied. This approach, however, can make the model over-parameterized. Hence orthonormal basis functions such as the Laguerre functions [23], [24] and Kautz functions [22], as well as generalized orthogonal basis (GOB) functions [25] are often selected to expand the Volterra kernels, and to reduce the parametric complexity. However, the use of these basis functions requires some knowledge of the poles of the system, and implementing them for higher-order MISO systems is quite exhaustive. In this work we treat the elements of Volterra kernels as individual parameters, and reduce the parametric complexity using proper orthogonal decomposition (POD) [26]. For the given input trace, the Volterra series input polynomials $\prod_{i=1}^{n} u(k-\tau_i)$ are expanded using orthogonal basis vectors. Since these orthogonal basis vectors are a linear combination of the Volterra input polynomial vectors, their coefficients are also the same linear combination of the elements of the Volterra series kernels. Based on energy considerations, a reduced subspace can be constructed for these orthogonal bases, and the model's projection onto this reduced subspace reduces the number of parameters to be estimated. Linear regression is then used to calculate these coefficients from the experimental data.

A third-order dual-input, single output (DISO) Volterra-series was established for the identification of the transient soot. The order of the model was kept low to avoid fitting noise, and the time-history of less than one second was used based on the cross-correlation results presented in Section 3. The two inputs (u_1 & u_2) were normalized by their maximum permitted values to get $\bar{u}_1, \bar{u}_2 \in [0, 1]$. As a result, the higher order terms can be neglected and soot is approximated as the sum of the first three orders of the output. The three orders of the output for this DISO system are calculated as shown in Eqns. 12-14, where the superscript of the Volterra kernel represents the input associated with the kernel.

Assuming the elements of each kernel are individual parameters, this results in a model with 470 parameters. In order to reduce the number of these parameters, the Volterra input polynomials in Eqns. 12-14 are arranged in the columns of A, with different rows corresponding to the data at different time samples. The columns of A are then mean centered and normalized by the standard deviation to scale the matrix and obtain $\bar{A}$. Singular value decomposition is then performed to obtain the orthogonal matrices U and V, and the matrix of singular values $\Sigma = diag(\sigma_1, \sigma_2, \ldots, \sigma_n)$ with $\sigma_1 \geq \sigma_2 \geq \ldots \geq \sigma_n \geq 0$, as $\bar{A} = U \Sigma V^T$.

The columns of the matrix $V_{470 \times 470}$ form an orthogonal basis of the state space for the traces of Volterra input polynomials, and the squares of the singular values provide a measure of how much signal energy is captured by each of these basis vectors. Let $\bar{H} = [\bar{h}_1, \bar{h}_2, \ldots, \bar{h}_{470}]$ be the vector of the coefficients of the orthogonal basis vectors, representing the linear combination of the elements of the Volterra kernels $H = [h_1, h_2, \ldots, h_{470}]$. Then, a reduced model is derived by considering only the first r bases of this subspace, spanned by the first r columns of matrix V, and denoted by V_r. The new basis vectors are then calculated by

$$y_1(k) = y_1^{u_1}(k) + y_1^{u_2}(k) = \sum_{n_1=1}^{2} \sum_{\tau=0}^{\varepsilon_n} h_1^{u_{n_1}}(\tau) \bar{u}_{n_1}(k-\tau) \tag{12}$$

$$y_2(k) = y_2^{u_1 u_1}(k) + y_2^{u_1 u_2}(k) + y_2^{u_2 u_2}(k) = \sum_{n_1=1}^{2} \sum_{n_2=n_1}^{2} \sum_{\tau_1=0}^{\varepsilon_n} \sum_{\tau_2=0}^{\varepsilon_n} h_2^{u_{n_1} u_{n_2}}(\tau_1, \tau_2) \bar{u}_{n_1}(k-\tau_1) \bar{u}_{n_2}(k-\tau_2) \tag{13}$$

$$\begin{aligned} y_3(k) &= y_3^{u_1 u_1 u_1}(k) + y_3^{u_1 u_1 u_2}(k) + y_3^{u_1 u_2 u_2}(k) + y_3^{u_2 u_2 u_2}(k) \\ &= \sum_{n_1=1}^{2} \sum_{n_2=n_1}^{2} \sum_{n_3=n_2}^{2} \sum_{\tau_1=0}^{\varepsilon_n} \sum_{\tau_2=0}^{\varepsilon_n} \sum_{\tau_3=0}^{\varepsilon_n} h_3^{u_{n_1} u_{n_2} u_{n_3}}(\tau_1, \tau_2, \tau_3) \bar{u}_{n_1}(k-\tau_1) \bar{u}_{n_2}(k-\tau_2) \bar{u}_{n_3}(k-\tau_3) \end{aligned} \tag{14}$$

projecting the system's model onto this subspace (Galerkin projection) as

$$\Phi = A V_r^T \tag{15}$$

It was observed that for all datasets, first 25 principal components captured 99.9% of the system's energy. Hence, r was chosen as 25. Let Y denote the time trace of the instantaneous soot recorded during experiments, $\bar{Y}$ the model estimate, and $\bar{H}_r = [\bar{h}_1, \bar{h}_2, \ldots, \bar{h}_r]$ the r coefficients of the reduced model, then $\bar{Y} = \Phi \bar{H}_r^T$, and the least-squares optimal solution for model identification, $\hat{H}_r$, is calculated as

$$\hat{H}_r = \arg\min_{\bar{H}_r} \|Y - \Phi \bar{H}_r^T\|_2 \tag{16}$$

V. Model Validation Results

This section presents the validation of the model based on Volterra series, and compares the results with steady-state maps. Identification of the model was performed on a number of different datasets, and model validation exercises was carried out on the others. Model estimates for the validation datasets were obtained by projecting the Volterra input polynomials of the respective sets onto V_r, and then multiplying them with the vector of new coefficients ($\hat{H}_r$) obtained during identification. It was observed that the identification done with highly transient datasets (conventional vehicle, downsized engine, parallel electric hybrid) improved the prediction accuracy during tip-in operations over steady-state maps. This is intuitive because when the driver presses the throttle in a drive-by-wire system, greater volume of fuel is injected into the cylinder to create more torque but the boost pressure lags behind due to turbocharger inertia, reducing the in-cylinder air-fuel ratios. The controller monitors this, and it limits the amount of fuel injected, nevertheless instantaneous excursions of air/fuel ratio and residual exhaust gas are quite probable. Additionally, the momentum of the incoming charge and the swirl intensity are reduced. This impedes the mixture preparation, and increases the heterogeneity of the mixture resulting in an overshoot in particulate and gaseous emissions [1], [2]. None of these effects are captured by the steady-state maps because they are not memory based, and hence fall short of accurate soot predictions during transients.

The predictions were, however, biased for the steady-state operation. This disparity can be explained by considering the physics of soot formation. Particle formation due to nucleation is predominant at low-load steady-state operations resulting in smaller spectral diameter of the particles. At transient loads, accumulation mode also contributes to the particle formation of bigger diameters [3], [1]. Since this Volterra series is identified using only FTP-75 data that contains limited amount of steady-state information, the predictions were slightly inaccurate. When identification was done using the data-set predominantly containing steady-state data (series hydraulic hybrid dataset), the bias at steady-state predictions was eliminated. In this case the accuracy over transient predictions deteriorated due to the lack of a sufficiently rich model during identification.

This problem was circumvented using datasets rich in both transient and steady-state information for identification. For this purpose, the conventional vehicle dataset was augmented by that of the series hydraulic hybrid, and coefficients were obtained that resulted in the least total error for both of these datasets. Validation was then performed on different datasets, including electric and hydraulic hybrids with different control strategies, all producing different time traces of the inputs. Fig. 7 shows the results for the validation of downsized engine data-set for part of the FTP-75 city cycle. The model estimates are compared with experimental data and quasi-steady state predictions obtained by using steady-state maps at the same inputs. As seen from the graph, the prediction accuracy with Volterra series improves substantially over the steady-state map during transients, whereas both the models match the experimental data at quasi steady-state operations. A more structured approach to model validation can be adopted by the statistical analysis of the residuals, defined as $R = Y - \bar{Y}$. If the model captures all the dominant dynamics of the system, the residuals should closely resemble white noise. Fig. 8 shows the autocorrelation of the residuals for this dataset. Also plotted is the 99% confidence interval for the autocorrelation of white noise containing an equal number of samples $(13,601)$. It can be seen that the residuals closely resemble white noise. Similar results are obtained for other validation datasets, and the model is considered validated.

The improvements in prediction accuracy over steady-state maps are measured in terms of L_2 error norms over the entire FTP-75 cycle. Fig. 9 shows the results of improvements for the different configurations (datasets different from identification datasets). It can be seen that the model estimates are about 17%, and 21% more accurate than the quasi steady

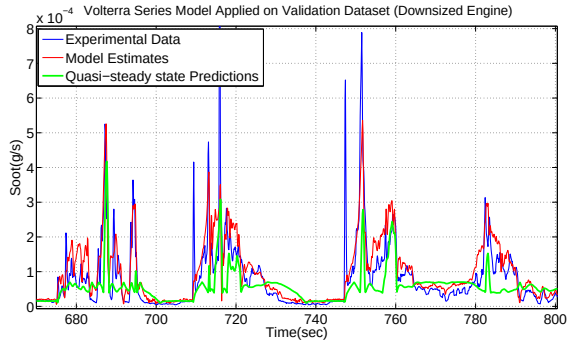

Fig. 7. VOLTERRA ESTIMATES FOR THE VALIDATION DATASET

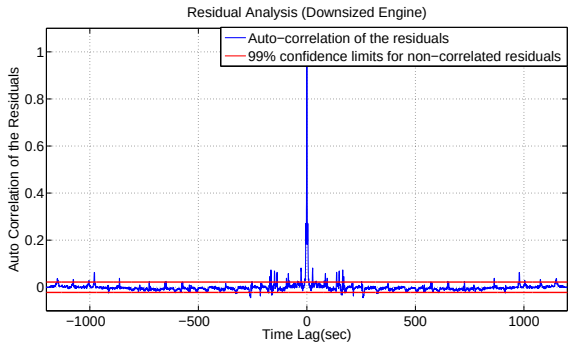

Fig. 8. RESIDUAL ANALYSIS FOR THE VALIDATION DATASET

state predictions for conventional vehicle and downsized engine, respectively. Improvements are much higher for the hybrids, 41% for the parallel electric and 27% for the series hydraulic, as engine tip-in becomes more frequent. Overall, the models estimate soot both qualitatively and quantitatively better than steady-state maps, and it does so by just using a 25 parameter third-order model, thus being computationally efficient and conducive to controls work.

VI. CONCLUSIONS

This work presented the development of black-box transient soot models using Volterra series with only two inputs ω_e and $\dot{m}$. Experimental data were recorded using numerous EIL experiments. Based on the data, a third-order 25 parameter discrete-time Volterra series was developed,

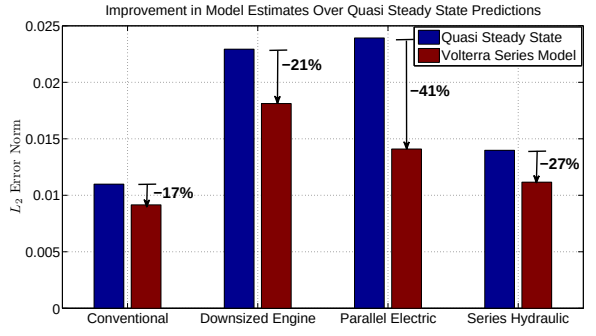

Fig. 9. REDUCTION IN L_2 ERROR NORMS FOR VOLTERRA MODELS

and validated. It was shown that the model estimated the transient soot significantly better than the steady-state maps, both qualitatively and quantitatively, while still remaining computationally efficient. Development of this model, thus provides a valuable tool required for the offline powertrain control system development of conventional and diesel hybrid vehicles.

VII. ACKNOWLEDGEMENT

We would like to acknowledge the help provided by Dr. Alexander Knalf, Ashwin Salvi, and Rajit Johri for test-cell data-acquisition and instrumentation, and Dhananjay Anand for his work with SISO soot models. We would also like to thank Dr. Emine Cagin, and Dr. Laura Brown for providing help on the manuscript.

REFERENCES

[1] Z. Filipi, J. Hagena, and H. Fathy, "Investigating the impact of in-vehicle transients on diesel soot emissions," *Thermal Science*, vol. 12, no. 1, pp. 53–72, 2008.

[2] C. D. Rakopoulos, A. M. Dimaratos, E. G. Giakoumis, and D. C. Rakopoulos, "Evaluation of the effect of engine, load and turbocharger parameters on transient emissions of diesel engine," *Energy Conversion and Management*, vol. 50, no. 9, pp. 2381–2393, 2009.

[3] J. R. Hagena, Z. S. Filipi, and D. N. Assanis, "Transient diesel emissions: Analysis of engine operation during a tip-in," in *SAE 2006 World Congress and Exhibition*, Detroit, MI, April, 2006.

[4] K. Tufail, P. Eastwood, T. Winstanley, S. Karagiogis, A. Darlington, Y. Hardalupas, and A. Taylor, "Deviations in emissions of NO and soot from steady-state, during transient operation of a common-rail diesel engine," in *9th International Conference on Engines and Vehicles*, Naples, Italy, September 2009.

[5] S. Hong, M. S. Wooldridge, H. G. Im, D. N. Assanis, and H. Pitsch, "Development and application of a comprehensive soot model for 3D CFD reacting flow studies in a diesel engine," *Combustion and Flame*, vol. 143, no. 1-2, pp. 11 – 26, 2005.

[6] X. Seykens, R. Baert, B. Somers, and F. Willems, "Experimental validation of extended NO and soot model for advanced HD diesel engine combustion," in *SAE World Congress & Exhibition*, Detroit, MI, April 2009.

[7] A. Westlund, "Fast physical emission predictions for off-line calibration of transient control strategies," in *SAE Powertrains, Fuels and Lubricants Meeting*, Florence, Italy, June 2009.

[8] J. Boulanger, F. Liu, W. S. Neill, and G. J. Smallwood, "An improved soot formation model for 3D diesel engine simulations," *Transactions of the ASME: Journal of Engineering for Gas Turbines and Power*, vol. 129, no. 3, pp. 877–84, July 2007.

[9] D. Jung and D. N. Assanis, "Quasidimensional modeling of direct injection diesel engine nitric oxide, soot, and unburned hydrocarbon emissions," *Transactions of the ASME: Journal of Engineering for Gas Turbines and Power*, vol. 128, no. 2, pp. 388–96, 04 2006.

[10] J. Zheng and Q. Xin, "Theoretical analysis of diesel engine NOx and soot with heuristic macro-parameter-dependent approach and virtual multi-zone real-time models," in *SAE Commercial Vehicle Engineering Congress & Exhibition*, Rosemont, IL, October 2009.

[11] Y. He and C. Rutland, "Application of artificial neural networks in engine modelling," *International Journal of Engine Research*, vol. 5, no. 4, pp. 281 – 296, 2004.

[12] H. K. Fathy, R. Ahlawat, and J. L. Stein, "Proper powertrain modeling for engine-in-the-loop simulation," in *2005 ASME International Mechanical Engineering Congress and Exposition*, vol. 74 DSC, Orlando, FL, United States, Nov 5-11 2005, pp. 1195–1201.

[13] J. Liu, J. Hagena, H. Peng, and Z. Filipi, "Engine-in-the-loop study of the stochastic dynamic programming optimal control design for a hybrid electric HMMWV," *International Journal of Heavy Vehicle Systems*, vol. 15, no. 2-4, pp. 309 – 26, 2008.

[14] Z. Filipi and Y. Kim, "Hydraulic hybrid propulsion for heavy vehicles: Combining the simulation and engine-in-the-loop techniques to maximize the fuel economy and emission benefits," *Oil & Gas Science and Technology - Revue de l'Institut Français du Pétrole*, vol. 65, no. 1, pp. 155–178, 2010.

[15] N. Collings, K. S. Reavell, and T. Hands, "A fast response particulate spectrometer for combustion aerosols," in *SAE Powertrain & Fluid Systems Conference & Exhibition*, San Diego, CA, October 2002.

[16] K. Yacoub, "Relationship between multiple and partial coherence functions," *IEEE Transactions on Information Theory*, vol. IT-16, no. 6, pp. 668 – 672, 1970.

[17] M. Canova, S. Midlam-Mohler, Y. Guezennec, G. Rizzoni, L. Garzarella, M. Ghisolfi, and F. Chiara, "Experimental validation for control-oriented modeling of multi-cylinder HCCI diesel engines," in *American Society of Mechanical Engineers, Dynamic Systems and Control Division*, Chicago, IL, United states, 2006.

[18] E. Bedrosian and S. Rice, "The output properties of volterra systems (nonlinear systems with memory) driven by harmonic and gaussian inputs," *Proceedings of the IEEE*, vol. 59, no. 12, pp. 1688 – 708, Dec 1971.

[19] S. Boyd and L. O. Chua, "Fading memory and the problem of approximating nonlinear operators with volterra series," *IEEE Transactions on Circuits and Systems*, vol. CAS-32, no. 11, pp. 1150–61, 11 1985.

[20] L. M. Li and S. A. Billings, "Discrete time subharmonic modelling and analysis," *International Journal of Control*, vol. 78, no. 16, pp. 1265–84, 11/10 2005.

[21] C. Seretis and E. Zafiriou, "Nonlinear dynamical system identification using reduced volterra models with generalised orthonormal basis functions," in *Proceedings of 16th American Control Conference*. Evanston, IL, USA: American Autom. Control Council, 4-6 June 1997 1997.

[22] A. da Rosa, R. Campello, and W. Amaral, "An optimal expansion of volterra models using independent kautz bases for each kernel dimension," *International Journal of Control*, vol. 81, no. 6, pp. 962–75, June 2008.

[23] R. Campello, G. Favier, and W. do Amaral, "Optimal expansions of discrete-time volterra models using laguerre functions," *Automatica*, vol. 40, no. 5, pp. 815–22, 2004.

[24] Q. Zheng and E. Zafiriou, "Volterra-laguerre models for nonlinear process identification with application to a fluid catalytic cracking unit," *Industrial and Engineering Chemistry Research*, vol. 43, no. 2, pp. 340–348, 2004.

[25] P. Heuberger, P. Van den Hof, and O. Bosgra, "A generalized orthonormal basis for linear dynamical systems," *IEEE Transactions on Automatic Control*, vol. 40, no. 3, pp. 451 – 65, 1995.

[26] T. Ersal, H. Fathy, D. Rideout, L. Louca, and J. Stein, "A review of proper modeling techniques," *Journal of Dynamic Systems, Measurement and Control*, vol. 130, no. 6, pp. 0 610 081–06 100 813, Nov. 2008.